Synthesis of Chain End Functionalized Multiple Hydrogen Bonded Polystyrenes and Poly(alkyl acrylates) Using Controlled Radical Polymerization

Brian D. Mather, Jeremy R. Lizotte, and Timothy E. Long*

Department of Chemistry, Virginia Polytechnic Institute and State University, Blacksburg, Virginia 24061-0344

Received May 28, 2004; Revised Manuscript Received September 8, 2004

ABSTRACT: Hydrogen bonding uracil functionalized polystyrenes and poly(alkyl acrylate)s were synthesized via stable free radical polymerization. Quantitative chain end functionalization was achieved using novel uracil containing TEMPO- and DEPN-based alkoxyamine unimolecular initiators. Polymerizations were conducted at 130 °C and yielded functionalized homopolymers with narrow molecular weight distributions ($M_w/M_n \sim 1.20$) and predictable molecular weights. Polymerizations of both *n*-butyl acrylate and styrene using the DEPN- and TEMPO-based alkoxyamines resulted in molecular weight control over a wide range of conversions. Terminal functionalization of poly(alkyl acrylate)s with hydrogen bonding groups increased the melt viscosity at temperatures below 80 °C, which was defined as the dissociation temperature, and as expected, the viscosity approached that of the nonfunctional analogues above this temperature. The hydrogen bonding effect was also evident in thermal (DSC) analysis and ^{1}H NMR spectroscopic investigations, and low molar mass polystyrenes exhibited glass transition temperatures that were consistent with a higher apparent molar mass. ^{1}H NMR spectroscopy confirmed the presence of a single hydrogen bonding group at the chain terminus, which was consistent with a well-defined initiation process for two families of novel alkoxyamines.

Introduction

Stable free radical polymerization (SFRP), which is often also described as nitroxide mediated polymerization (NMP), is well established as a controlled radical polymerization methodology.[1−4] In a fashion similar to other controlled radical polymerization methodologies, the process relies on an equilibrium between dormant propagating chains and a low concentration of propagating radicals. The relatively high rate of initiation compared to propagation and the reduction of transfer or termination events through reversible capping of the growing radical chain end has led to the classification of this polymerization methodology as "living". The systematic variation of the monomer weight to the moles of initiator leads to predictable molecular weights and relatively low polydispersities ($M_w/M_n \sim 1.20$). Stable free radical polymerization offers functional group tolerance, which is typical of radical polymerizations. This tolerance provides versatility that is often not easily achieved with other living polymerization techniques, and less stringent purification techniques are required compared to living anionic polymerization. Moreover, stable free radical polymerization[1−4] enables the synthesis of block,[5] graft, star,[6,7] and hyperbranched[8] topologies in a fashion similar to other living polymerization processes.

Rizzardo et al. initially described stable free radical polymerization,[9,10] and later Georges et al. examined bimolecular initiators which primarily involved TEMPO (2,2,6,6-tetramethylpiperidinyloxy), conventional radical initiators (AIBN, BPO), and styrenic monomers.[11] This method proved very effective for styrenic monomers. Furthermore, the typical reaction rates initially were quite slow, and often days were required to reach high conversion. More recently, other monomers such as acrylates, dienes, and acrylamides were successfully polymerized using nitroxides such as DEPN (*N-tert*-butyl-*N*-(1-diethylphosphono-2,2-dimethylpropyl)-*N*-oxyl), which contains a hydrogen alpha to the nitroxide functionality.[12−15] Polymerizations, which utilized this family of nitroxides, exhibited greater propagation rates than the styrene/TEMPO systems, and this observation was attributed to the lower C−ON bond strengths due to steric strain.[15] Other factors such as nitroxide decomposition and thermal initiation play roles in the kinetics of stable free radical polymerizations, and efforts to minimize both competing mechanisms have received significant attention in the earlier literature and this current work.

Stable free radical polymerization is a premier method for obtaining chain end functionality due to recent advances in alkoxyamine "unimolecular" initiator synthesis. Unimolecular initiators have an added advantage over bimolecular initiator systems due to defined stoichiometry between the initiating fragment and the nitroxide. This feature leads to better control of molecular weight and polydispersity,[16] and many synthetic methods were discovered earlier for the preparation of alkoxyamine unimolecular initiators. For example, Wu et al. conducted a radical capping reaction between AIBN initiated styrene and TEMPO.[17] An alternate method involved hydrogen abstraction from benzylic sites using *tert*-butyl peroxide and in-situ radical capping with nitroxide.[16] Hawker[18] and Schmidt-Naake[19] have employed manganese complexes, e.g. Jacobsen's catalyst, to directly react styrene olefinic sites with nitroxides. Moreover, in a scheme that is reminiscent of atom transfer radical processes, nitroxides also react with an activated halide through a copper promoted coupling reaction.[13,20] The particular functionality of interest in our work was multiple hydrogen bonding chain end functionality, which was easily accessed using earlier synthetic strategies for unimolecular initiators.

10.1021/ma048938q CCC: $27.50
Published on Web 11/16/2004

Multiple hydrogen bonding has recently gained attention in the field of macromolecular and supramolecular chemistry due to the pioneering work of Meijer,[21] Stadler,[22] Lehn,[23] and others.[24,25] The use of multiple hydrogen bonding sites in conjunction with conventional oligomers and polymers has resulted in thermoreversible mechanical and rheological properties which are tunable based on the strength of the hydrogen bond.[24,25] For example, Meijer introduced a self-complementary 2-ureido-4[1*H*]-pyrimidone quadruple hydrogen bonding array at the ends a trifunctional oligomeric poly(propylene glycol-*co*-ethylene glycol) copolymer, and a thermoreversible network with film forming capability and elastomeric mechanical properties was observed.[21] Long[24] and Coates[26] have also investigated the introduction of pyrimidones in a random fashion in a copolymer using both radical and coordination polymerization methods, respectively. The hydrogen bonding motif offers unique thermoreversibility, and the influence on physical properties is quite evident in melt rheology. This design strategy offers promise for improved melt processability with equivalent polymer properties at temperatures below hydrogen bond dissociations and also enables potentially recyclable thermoreversible networks.

In biological systems, hydrogen bonding plays an essential role in protein folding and in maintaining the structure of DNA and RNA. For example, the reversibility of the hydrogen bonds that are between base pairs in the DNA structure allows for required unzipping in the transcription process.[27] In protein folding, hydrogen bonds establish the α-helix and β-sheet secondary structures. Introduction of nucleic acid base pairs (adenine, thymine, uracil, guanine, cytosine) into polymers is achievable via numerous means such as postpolymerization end group functionalization of well-defined anionically synthesized polymers[28] or conventional radical polymers,[29] synthesis of functionalized (meth)acrylic or vinyl monomers followed by conventional radical homopolymerization[30] or copolymerization,[31,32] alternating radical polymerization with maleic anhydride,[33] living cationic and anionic ring-opening polymerization of cyclic base pair derivatives,[34] or postpolymerization functionalization of poly(ethylene imine) and polypeptides.[35] The incorporation of base pairs leads to molecular recognition ability,[29,30] metal ligation,[32] photo-cross-linking (thymine),[30] photoresists,[30,36] and selective chromatographic media.[30]

The present work, which involves controlled radical polymerization, offers the advantage of controlled molecular weights and uracil placement without strenuous anionic techniques or potentially incomplete postpolymerization modification. Hydrogen bonding units that are comprised of the uracil nucleic acid base are introduced into styrenic and acrylic polymers using a new family of functionalized initiators. The expected self-association of these units was probed using a number of techniques, including melt rheology and ^{1}H NMR spectroscopy.

Experimental Section

Materials. Copper powder (45 μm, 99%), copper(II) triflate (98%), and 2,2,6,6-tetramethylpiperidinyloxy (TEMPO, 98%) were obtained from Acros and used as received. Copper(I) bromide (99.999%), 4,4′-dinonylbipyridine (dNbpy, 97%), and 6-chloromethyluracil (98%) were obtained from Aldrich and used as received. Styrene (99%, Aldrich), *n*-butyl acrylate (99%, Aldrich), dimethyl sulfoxide (DMSO, 99.9%, Aldrich), dimethylformamide (DMF, 99%, EM Science), and *N,N,N′,N″,N″*-pentamethyldiethylenetriamine (PMDETA, 99%, Aldrich) were distilled from calcium hydride and stored under nitrogen at 0 °C. DEPN was synthesized according to a procedure in the earlier literature.[15,37]

Synthesis of Uracil−TEMPO Unimolecular Initiator. 6-Chloromethyluracil (1.69 g, 10.5 mmol), TEMPO (1.64 g, 10.4 mmol), and dNbpy (170 mg, 0.42 mmol) were dissolved in dimethyl sulfoxide (DMSO, 10 mL). Dichloromethane (20 mL) and THF (10 mL) were added to the reaction mixture. The solution was subjected to three freeze−pump−thaw degassing cycles, warmed to room temperature, and cannulated into a nitrogen filled flask containing a stir bar, copper(II) triflate (37 mg, 0.10 mmol), and copper powder (0.670 g, 10.6 mmol). The reaction mixture was heated to 70 °C and stirred vigorously for 24 h. The contents of the reaction were precipitated into water, gravity filtered, and washed with water. The resultant product was dissolved in acetone and purified using flash chromatography on a silica column. The acetone was removed using rotary evaporation, and the product was dried under high vacuum at room temperature for 24 h. Uracil−TEMPO was obtained as a white solid (mp 205−207 °C) in 24% yield. ^{1}H NMR (400 MHz, $CDCl_3$): 1.1−1.6 ppm (br multiplet, 18H from TEMPO including methyls at 1.1 ppm), 4.6 ppm (d, J = 1.2 Hz, N−O−CH_2−C=C: 2H), 5.6 ppm (br s, C=C*H*-C=O: 1H), 8.5 ppm (br, N−*H*: 2H). ^{13}C NMR (100 MHz, DMSO-d_6): 16.9 ppm, 20.3 ppm, 31.2 ppm, 32.8 ppm (TEMPO 2° and 1° carbons), 60.1 ppm (TEMPO quaternary carbons), 73.6 ppm (*C*H$_2$−O−N), 96.8 ppm (C=*C*H−C=O), 151.8 ppm (NH−*C*=O−NH), 153.0 ppm (*C*=CH−C=O), 164.5 ppm (C=CH−*C*=O). FAB MS: m/z = 282.1794 amu (experimental), m/z = 282.1818 amu (theoretical).

Synthesis of Uracil−DEPN Unimolecular Initiator. 6-Chloromethyluracil (1.82 g, 11.4 mmol), DEPN (3.00 g, 10.2 mmol), and PMDETA (3.51 g, 20.4 mmol) were dissolved in DMSO (20 mL). Dichloromethane (40 mL) was added to the reaction mixture. The solution was subjected to three freeze−pump−thaw degassing cycles, warmed to room temperature, and transferred under nitrogen into a nitrogen-filled flask containing a stir bar, copper(I) bromide (1.16 g, 8.2 mmol), and copper powder (0.51 g, 8.2 mmol). The reaction mixture was stirred vigorously for 24 h at ambient temperature. Dichloromethane (300 mL) was added to the reaction mixture, and the contents were washed with deionized water five times, dried over sodium sulfate, and decanted. The solvent was removed using rotary evaporation at ambient temperature, and the resulting green oil was subjected to column chromatography on silica and eluting with acetone. The acetone was removed using rotary evaporation, and the product was dried under high vacuum at room temperature for 24 h. Uracil−DEPN was obtained as a white solid (mp 137−141 °C) in 71% yield. ^{1}H NMR (400 MHz, $CDCl_3$): 1.16 ppm (two s, two C(CH_3)$_3$: 18H), 1.2−1.36 ppm (m, ethoxy CH_3: 6H), 3.30 ppm (d, J_{P-H} = 25 Hz −N−C*H*C(CH$_3$)$_3$−PO(OEt)$_2$: 1H), 3.95−4.22 ppm (m, ethoxy CH_2: 4H), 4.37 ppm and 4.91 ppm (two d, J = 11 Hz, C*H*$_2$−O−N: 2H), 5.48 ppm (br s, C=C*H*−C=O: 1H), 8.31 ppm (br, C−N*H*−C=O), 11.79 ppm (br, O=C−N*H*−C=O: 1H). ^{13}C NMR (100 MHz, $CDCl_3$): 16.2 ppm (ethoxy CH_3), 27.7 ppm (N−C(*C*H$_3$)$_3$), 30.3 ppm (C−C(*C*H$_3$)$_3$), 36.3 ppm (C−*C*(CH$_3$)$_3$), 60.3 ppm, 61.7 ppm (P−O−*C*H$_2$, J_{C-P} = 144 Hz), 62.5 (N−*C*(CH$_3$)$_3$), 67.6 ppm and 69.0 ppm (N−*C*H−P, J_{C-P} = 140 Hz), 73.5 ppm (*C*H$_2$−O−N), 99.6 ppm (C=*C*H−C=O), 150.0 ppm (NH−*C*=O−NH), 151.1 ppm (*C*=CH−C=O), 164.2 ppm (C=CH−*C*=O). FAB MS: m/z = 420.2271 amu (experimental), m/z = 420.2263 amu (theoretical).

Polymerizations of Styrene Using Uracil−TEMPO. A 100 mL round-bottomed flask containing a magnetic stirring bar was charged with Uracil−TEMPO (100 mg, 0.35 mmol), sealed with a septum-capped three-way glass adaptor connected to a vacuum line, and flushed through repeated vacuum/nitrogen cycles before distilled styrene monomer (30 mL, 259 mmol) was introduced via syringe. The solution was further degassed with multiple freeze−pump−thaw cycles using a dry ice/2-propanol bath and warmed to room temperature. The in-situ FTIR probe was inserted into a 100 mL

three-necked flask, and the system was septum sealed and flushed with nitrogen for 30 min. The degassed solution was transferred under an inert atmosphere into the three-necked flask and immersed in an oil bath, which was maintained at 130 °C. Samples (2−3 mL) were removed from the reaction at hourly intervals using a syringe. All samples, as well as the final product, were isolated by precipitation into a large excess of 2-propanol after first diluting with an equal volume of THF and followed by drying overnight under vacuum at elevated temperature (∼80−100 °C). The final polymer product had M_n = 47 200 and M_w/M_n = 1.22 as determined by GPC MALLS, which agrees well with the molecular weight calculated on the basis of monomer conversion as measured using in-situ FTIR spectroscopy (47100, 62% conversion).

Polymerizations of *n*-Butyl Acrylate Using Uracil−DEPN. Polymerizations involving *n*-butyl acrylate and Uracil−DEPN were conducted in an analogous fashion to those involving styrene and Uracil−TEMPO; however, an additional 0.5 equiv of DEPN was added to the reaction mixture prior to degassing. A small excess of nitroxide was shown earlier to be necessary for improved control of nitroxide mediated acrylate polymerizations.[38,39] Uracil−DEPN initiator (120 mg, 0.29 mmol) and DEPN (42 mg, 0.14 mmol) were added to a 100 mL round-bottom flask containing a magnetic stirring bar. The flask was sealed with a septum capped three-way glass adaptor, connected to a vacuum line, and flushed through repeated vacuum/nitrogen cycles before distilled *n*-butyl acrylate monomer (28.5 mL, 200 mmol) and distilled DMF (10 mL) were introduced via syringe. The solution was further degassed with multiple freeze−pump−thaw cycles using a dry ice/2-propanol bath and warmed to room temperature. The in-situ FTIR probe was inserted into a 100 mL three-neck flask, and the system was septum sealed and flushed with nitrogen for 30 min. The degassed solution was transferred under a nitrogen atmosphere into the three-necked flask and immersed in an oil bath, which was maintained at 130 °C. Samples (2−3 mL) were removed from the reaction at hourly intervals using a syringe. All samples, as well as the final product, were isolated by precipitation into a large excess of methanol/water (9:1) and subsequently vacuum-dried overnight at elevated temperature (∼80−100 °C). The final polymer product had M_n = 44 600 and M_w/M_n = 1.17 as determined by GPC MALLS, which agrees well with the molecular weight calculated from monomer conversion (42 700, 48% conversion).

Polymer Characterization. Gel permeation chromatography (GPC) was performed at 40 °C in chloroform or THF at a flow rate of 1 mL/min using a Waters size exclusion chromatographer equipped with an autosampler, three 5 μm PLgel Mixed-C columns, a Waters 2410 refractive index (RI) detector operating at 880 nm, and a miniDAWN multiangle laser light scattering (MALLS) detector operating at 690 nm, which was calibrated with polystyrene standards. The refractive index increment (d*n*/d*c*) was calculated online. GPC of uracil−polystyrenes in *N*-methylpyrrolidone containing 0.05 M LiBr was performed using a Waters size exclusion chromatographer equipped with a 2414 refractive index detector, which was calibrated using polystyrene standards. Variation of solvent did not appear to result in significant differences in terms of elution behavior of uracil functionalized polymers and will be discussed later. In-situ FTIR spectroscopic analysis was performed using an ASI ReactIR 1000 attenuated total reflectance (ATR) spectrometer.[40−44] Differential scanning calorimetry (DSC) was performed under a nitrogen flush at a heating rate of 10 °C/min on a PE Pyris 1 instrument, which was calibrated using indium (mp = 156.60 °C) and zinc (mp = 419.47 °C) standards. Glass transition temperatures were measured as the midpoint of the transition. Thermogravimetric analysis (TGA) was performed under a nitrogen atmosphere at a heating rate of 10 °C/min using a TA Instruments Hi-Res TGA 2950. NMR spectroscopic data were collected in either $CDCl_3$ or DMSO-d_6 on a Varian 400 MHz spectrometer at ambient temperature. Melt rheology was performed on a stress-controlled TA Instruments Advanced rheometer 1000 using a 1 kPa oscillatory stress and a 62.45 rad/s shear rate in a 25 mm diameter parallel plate geometry with a plate separation distance of 1 mm.

Scheme 1. Synthetic Scheme for Uracil−TEMPO Unimolecular Initiator Synthesis and Subsequent Polystyrene Polymerization

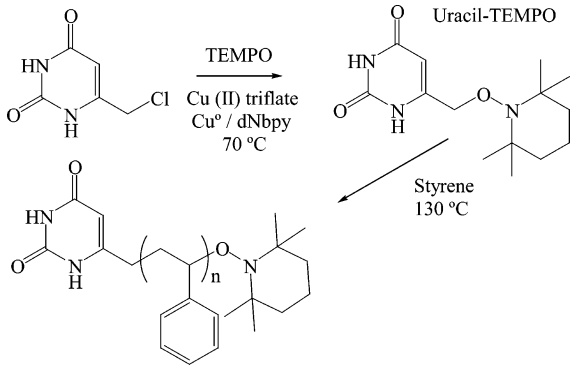

Scheme 2. Synthetic Scheme for Uracil−DEPN Unimolecular Initiator Synthesis and Subsequent Poly(*n*-butyl acrylate) Polymerization

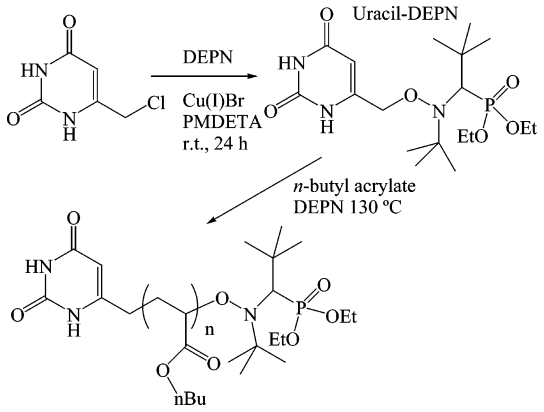

Results and Discussion

Uracil−TEMPO and Uracil−DEPN Unimolecular Initiator Syntheses. The Uracil−TEMPO unimolecular initiator was synthesized analogously to non-hydrogen-bonding alkoxyamines discussed in the literature (Scheme 1).[20] A copper(I) species, which is generated from Cu^0 and copper(II) triflate, reductively cleaves the C−Cl bond in 6-chloromethyluracil, and TEMPO efficiently caps the resulting allylic radical in solution. A similar approach was used for Uracil−DEPN synthesis; however, copper(I) bromide was introduced rather than generated in situ (Scheme 2).[13] These synthetic methods are convenient but are limited to activated halides, such as benzylic halides or α-halocarbonyl compounds, due to the instability of the radical generated from nonactivated alkyl halides. In this work, it was demonstrated that the conjugated enone activates the chloride on 6-chloromethyluracil and enables the one-step synthesis of a unimolecular initiator containing a site for hydrogen bonding.

Polymerizations of Styrene and *n*-Butyl Acrylate Using the Uracil-Based Initiators. Polystyrenes and poly(*n*-butyl acrylates) with molecular weights ranging from 4500 to 42 000 with narrow molecular weight distributions were synthesized using Uracil−TEMPO and Uracil−DEPN. The polymerization reactions were colorless and exhibited significant increases in viscosity but typically were not allowed to vitrify. The polymer products were colorless and similar in appearance to polymers that were prepared using conventional azo or peroxide initiators. In some experiments, polymerizations were performed using 25 vol % DMSO or

Table 1. Target and Experimental Molecular Weights for Polystyrenes and Poly(*n*-butyl acrylate)s Synthesized Using Uracil−TEMPO and Uracil−DEPN

monomer/initiator	target[a] M_n	GPC[b] M_n	M_w/M_n
styrene/U-TEMPO	7 100	8 000	1.10
styrene/U-TEMPO	13 200	13 000	1.27
styrene/U-TEMPO	27 000	25 200	1.26
styrene/U-TEMPO	36 500	39 800	1.26
styrene/U-TEMPO	43 700	45 700	1.21
styrene/U-TEMPO	69 900	75 200	1.27
styrene/U-TEMPO	84 400	99 200	1.28
nBA/U-DEPN	4 100	5 900	1.20
nBA/U-DEPN	9 100	9 800	1.22
nBA/U-DEPN	11 700	13 700	1.12
nBA/U-DEPN	19 500	19 100	1.12
nBA/U-DEPN	27 000	26 100	1.11
nBA/U-DEPN	35 600	33 300	1.18
nBA/U-DEPN	42 500	44 600	1.17

[a] Target = % conversion × ($g_{monomer}$/$moles_{init}$) (conversion measured using in-situ FTIR). [b] MALLS, 40 °C.

Table 2. Uracil Functionalized Polystyrene and Poly(*n*-butyl acrylate) Molecular Weights Determined Using Both GPC and NMR

monomer/initiator	GPC[a] M_n	NMR[b] M_n	M_w/M_n
styrene/U-TEMPO	4 500	4 800	1.07
styrene/U-TEMPO	7 800	7 000	1.04
styrene/U-TEMPO	10 500	9 400	1.04
styrene/U-TEMPO	14 600	14 400	1.05
styrene/U-TEMPO	21 600	21 500	1.26
nBA/U-DEPN	5 900	5 500	1.20
nBA/U-DEPN	13 700	13 400	1.12
nBA/U-DEPN	16 700	15 300	1.09
nBA/U-DEPN	19 100	21 000	1.12
nBA/U-DEPN	26 100	28 500	1.11
nBA/U-DEPN	33 000	33 800	1.14
nBA/U-DEPN	40 600	48 800	1.19

[a] MALLS, 40 °C. [b] 400 MHz, $CDCl_3$, rt, using uracil alkene proton.

DMF to study the effect of hydrogen bond screening solvents on the polymerization; however, statistically significant effects on the kinetics or the molecular weight evolution with conversion were not observed.

Good agreement was obtained between experimental molecular weights and molecular weights calculated from monomer conversion as measured using in-situ FTIR spectroscopy ($g_{styrene}$/$mol_{initiator}$ × % conversion) (Table 1). Typically, low conversions (∼50%) were targeted due to the risk of side reactions at higher conversion such as nitroxide degradation and chain termination which can lead to broadened polydispersities.[45] ^{1}H NMR spectroscopy was utilized to verify the presence of the uracil end group through comparison of the NMR number-average molecular weights with GPC results (Table 2). In the case of polystyrenes, the ratio of the integration of the aromatic protons to the integration of the alkene proton of the uracil end group allowed the accurate calculation of NMR number-average molecular weights for values less than 25 000. For poly(*n*-butyl acrylate)s, the ratio of the integration of the CH_2 protons that are α to the acrylate ester to the integration of the alkene proton of the uracil end group was used to calculate molecular weights. Similar calculations were performed using protons α to the nitroxide end groups, and comparable results were obtained. In the case of uracil functionalized polystyrenes, ^{1}H NMR spectroscopy also allowed the verification of TEMPO methyl resonances near 0.5 ppm.

In-Situ FTIR Monitoring of Polymerization Kinetics. In-situ FTIR spectroscopy is a powerful, state-of-the-art analytical technique for monitoring numerous organic reactions. The primary strengths of this technique include kinetic analyses, determining reaction order, and obtaining real-time conversion information. The ASI ReactIR instrument is equipped with a diamond composite/stainless steel probe, which allows the monitoring of reactions under a wide range of pressures (up to 100 psi), temperatures (up to 300 °C), and aggressive reagents. Our research laboratories have devoted significant attention to the kinetic analyses of nitroxide mediated polymerization using in-situ FTIR spectroscopy.[40−44]

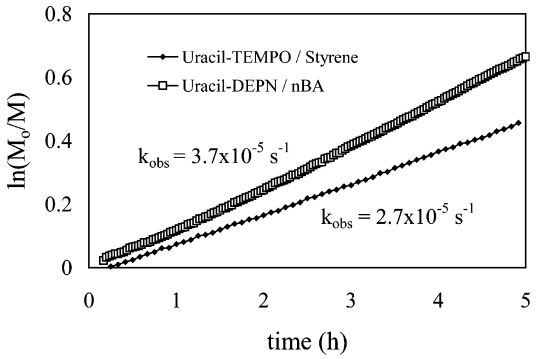

Figure 1. In-situ FTIR kinetic plot of styrene and *n*-butyl acrylate polymerizations at using Uracil−TEMPO and Uracil−DEPN at 130 °C. [Styrene]:[U-TEMPO] = 1460 (bulk), [nBA]:[U-DEPN] = 695 (25 vol % DMSO).

Table 3. Polymerization Rate Constants for Various Styrene to Uracil−TEMPO Ratios

moles of monomer:moles of initiator	k_{obs}[a] (s^{-1})
366:1	3.02×10^{-5}
488:1	3.12×10^{-5}
732:1	2.97×10^{-5}
1460:1	2.69×10^{-5}
1740:1	3.06×10^{-5}

[a] Determined by in-situ FTIR, 130 °C.

The polymerization kinetics of styrene and *n*-butyl acrylate using the uracil based initiators at 130 °C revealed pseudo-first-order polymerization kinetics, which is expected for radical polymerizations and is indicative of a constant number of propagating centers (Figure 1). The absorbance at 907 cm^{-1}, which corresponds to the vinyl CH_2 wag of styrene, was used to determine the styrene concentration based on a calibration curve that was constructed from a range of styrene/polystyrene compositions at 130 °C. The average observed rate constant ($k_{obs} = k_p[R^•]$) for Uracil−TEMPO initiated styrene polymerization of approximately 3.0×10^{-5} s^{-1} was 50% higher than literature values for TEMPO mediated polymerization of styrene at 132 °C using a similar method.[44] It is possible that this difference arises from the use of a unimolecular initiating system in this work as opposed to the bimolecular reaction previously employed since stoichiometric mismatch in the latter case could lead to excess nitroxide. Furthermore, the use of a calibration curve in analyzing the in-situ FTIR spectroscopic data may have also contributed to this difference since calibration was not used in the cited reference. Interestingly, for various ratios of Uracil−TEMPO to styrene, nearly identical rate constants were obtained (Table 3), which is consistent with the observations of Fischer[46] and others,[47] that the amount of initiator did not affect the polymerization rate. Similar

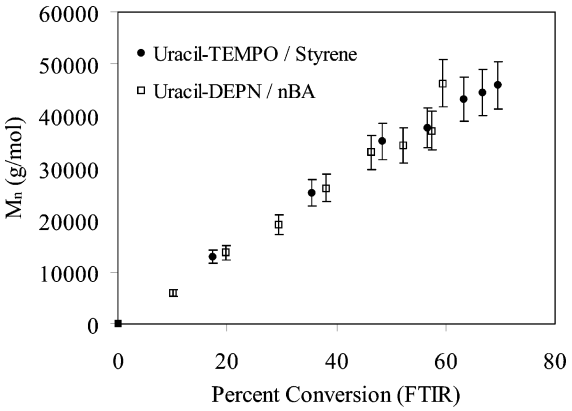

Figure 2. Evolution of molecular weight with conversion for the polymerizations of styrene and *n*-butyl acrylate from Uracil−TEMPO and Uracil−DEPN at 130 °C with 25 vol % DMSO. [Styrene]:[U-TEMPO] = 730, [nBA]:[U-DEPN] = 695.

equilibrium concentrations of active radicals exist in these polymerizations; however, these active radicals are in equilibrium with differing numbers of dormant chains, which leads to different molecular weights at various [M]:[I] ratios.

During in-situ FTIR spectroscopic investigations of the *n*-butyl acrylate polymerizations, calibration curves were obtained for known mixtures of *n*-butyl acrylate and poly(*n*-butyl acrylate) at an absorbance maximum centered at 968 cm^{-1}. The rate constant of polymerization of *n*-butyl acrylate using the Uracil−DEPN unimolecular initiator in DMSO was 3.7×10^{-5} s^{-1} at an initiator concentration of 7.4 mM. This rate constant appears low considering that DEPN-based styrene polymerizations were shown earlier to proceed at significantly faster rates than analogous TEMPO mediated polymerizations.[37] Faster rate constants were reported for *n*-butyl acrylate polymerizations at a lower temperature (120 °C) without additional DEPN ($\sim 1 \times 10^{-4}$ s^{-1}).[38] It is presumed that the slower kinetics in this work is due to the introduction of 0.5 equiv of additional nitroxide relative to initiator into the polymerizations, which is known to slow polymerization kinetics.[12,39]

The evolution of molecular weight with conversion was obtained through a combination of sampling techniques and in-situ FTIR spectroscopy (Figure 2). In the case of both unimolecular initiators, number-average molecular weights increased in proportion to monomer conversion, with a proportionality constant equal to grams of monomer divided by moles of initiator.

Characterization of Hydrogen Bonding Using ^{1}H NMR Spectroscopy. Dilution affects the position of the equilibrium between individual and associated hydrogen bonding groups in the system, as is suggested in the definition of the association constant.[48] Diluting a system composed of associating species should shift the equilibrium toward the unassociated species. Thus, changing the concentration of the uracil end group in $CDCl_3$ induced a change in the degree of hydrogen bonding which resulted in a change in the chemical shift of one of the N−H protons. Rather than changing the concentration of the polymer in solution, samples of uracil functionalized polystyrene of different molecular weights were dissolved in chloroform-*d* at an identical concentration of 10.4 wt %. This relatively high solution concentration was chosen due to the ease of observing the N−H protons in ^{1}H NMR spectroscopy as concentration increases. As the molecular weight of the polystyrenes increased, the chemical shift decreased, which indicated less hydrogen bonding interaction for the higher molecular weight polymer chains due to the lower chain end concentration (Figure 3). Attempts to fit the chemical shift vs concentration data to dimeric self-association models were unsuccessful, which suggested a higher stoichiometry for the complex.[49] However, the trend permitted the construction of a calibration curve for prediction of molecular weights for these polymers based on ^{1}H NMR spectroscopy. The uracil group is known to associate in several possible geometries due to the presence of both imide and lactam units in the uracil ring.[50] This is expected to lead to an association constant that reflects a combination of several complexes, but this should not hinder the measurement of the association constant.

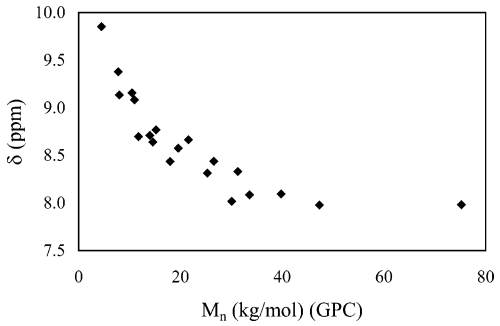

Figure 3. Chemical shift of uracil N−H protons as a function of molecular weight in $CDCl_3$ at 10.4 wt %.

Earlier observations of associations during GPC analysis for hydrogen bonding polymers has prompted GPC in more polar eluents.[51] Comparison of GPC measurements of uracil polystyrenes in NMP containing LiBr, a hydrogen bond screening agent, versus chloroform suggested that significant hydrogen bonding did not occur during the GPC analysis. Furthermore, the agreement of the GPC molecular weight data with target molecular weights as well as those obtained via NMR spectroscopic analysis suggests the absence of associations at the concentrations employed in GPC.

Characterization of Hydrogen Bonding Using Melt Rheology. The low glass transition temperature of poly(*n*-butyl acrylate) permits melt rheology experiments over a temperature range that spans both associated and dissociated states of the hydrogen bonding group, as the thermal dissociation of hydrogen bonding groups may occur at temperatures from 50 to 130 °C.[24,25,52,53] Melt rheology was performed on two samples of poly(*n*-butyl acrylate), one possessing the uracil end group (M_n = 25 400, M_w/M_n = 1.17) and another possessing a 1-phenylethyl group (M_n = 24 000, M_w/M_n = 1.16). Zero shear viscosities were collected over a temperature range from 20 to 100 °C (Figure 4). Melt viscosity enhancements were clearly observed for the uracil functionalized polyacrylate with nearly equivalent molecular weight. However, there was a stronger temperature dependence for the melt viscosity of the uracil functionalized poly(*n*-butyl acrylate), and dissociation of the hydrogen bonding groups appeared near 80 °C. An Arrhenius analysis of the zero shear viscosities revealed a higher flow activation energy for the uracil functionalized acrylate (54 kJ/mol vs 48 kJ/mol) (Figure 5). The correlation coefficient for the linear fit used to calculate the activation energy was 0.996 in both cases. On the basis of the fact that flow activation energy is independent of molecular weight,[54] the data

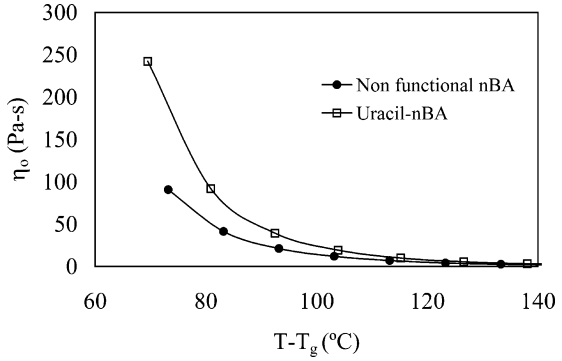

Figure 4. Zero shear melt viscosities for uracil functionalized poly(*n*-butyl acrylate) (M_n = 25 400, M_w/M_n = 1.17) and nonfunctionalized poly(*n*-butyl acrylate) (M_n = 24 000, M_w/M_n = 1.16).

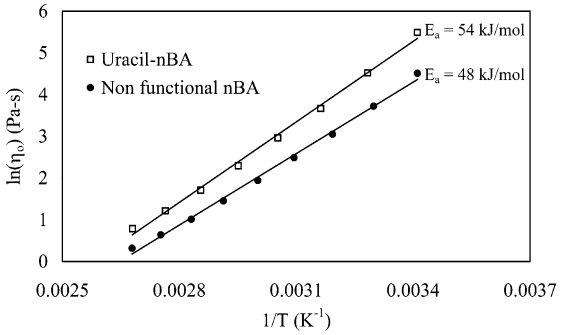

Figure 5. Arrhenius analysis of the melt rheology data depicting the flow activation energies for functionalized and nonfunctionalized poly(*n*-butyl acrylate).

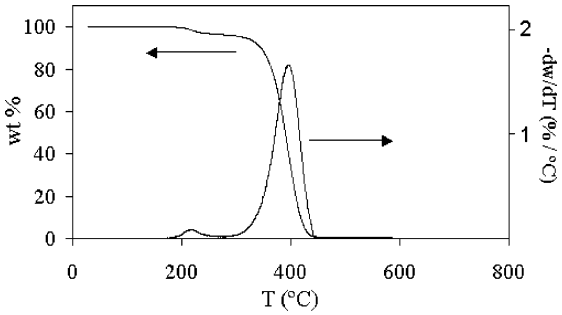

Figure 6. Thermogravimetric and derivative traces for a uracil functionalized polystyrene (M_n = 4500, M_w/M_n = 1.07).

suggest a more than dimeric association of the uracil end groups.

Thermal Analysis of Uracil Polystyrenes. Thermogravimetric analysis (TGA) was performed on the lower molecular weight uracil functionalized polystyrene samples (M_n < 15 000). A two-step degradation process was observed in each case (Figure 6). The weight loss during the first step (195−250 °C) decreased with increasing molecular weight. A two-step degradation process is not normally observed with nonfunctional polystyrene but was reported earlier for TEMPO functionalized polystyrene at similar temperatures.[55] To determine whether the first stage degradation involved the loss of TEMPO, an isothermal degradation experiment was performed in which a uracil functionalized polystyrene (M_n = 7800, M_w/M_n = 1.04, GPC MALLS) was heated to 230 °C for 30 min under nitrogen inside the TGA furnace. The sample remained completely soluble in $CDCl_3$, but a slightly brown color developed, and the ^{1}H NMR spectrum (Figure 7) indicated the

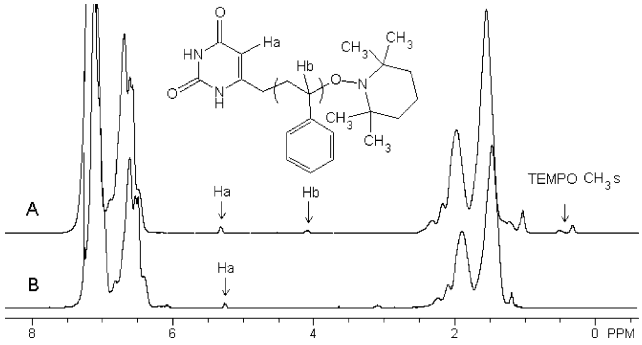

Figure 7. ^{1}H NMR spectra of a uracil functionalized polystyrene before (A) and after (B) pyrolysis under nitrogen at 230 °C. Arrows indicate the uracil alkene proton (5.4 ppm), the benzylic proton next to the nitroxide (4.1 ppm), and the peaks due to TEMPO methyl groups (0.5 ppm).

Table 4. Glass Transition Temperatures for Various Uracil Functionalized Polystyrenes with Molecular Weights below the Critical Molecular Weight

M_n (GPC[a])	T_g[b] (°C)
4 500	101
7 800	102
10 500	102
14 600	101

[a] MALLS, $CHCl_3$, 40 °C. [b] DSC: 10 °C/min, N_2, second heat.

presence of the uracil group in the polymer (the uracil alkene proton at 5.4 ppm) and the loss of the TEMPO group (the geminal dimethyl protons at 0.5 ppm and benzylic ether proton at 4.1 ppm). The molecular weight calculated using the uracil alkene proton peak (M_n = 7500) was similar to the value obtained from ^{1}H NMR spectroscopy before degradation (M_n = 7000). Gel permeation chromatography showed that the molecular weight had increased slightly and that the distribution had also broadened (M_n = 8100, M_w/M_n = 1.27), possibly due to coupling events. A resonance in the spectrum for the degraded polymer at 3.1 ppm likely represents benzylic protons at head to head linkages formed during styrenic radical combination.[55]

A series of uracil functionalized polystyrenes with molecular weights between 5000 and 15 000 were subjected to DSC analysis in order to determine their glass transition temperatures. All samples had approximately the same glass transition temperature (Table 4), despite the fact that molar masses were below 15 000, where nonassociating end groups typically contribute to a lower glass transition temperature.[56] Lin has demonstrated that the glass transition temperature of polystyrene decreases markedly as a function of molar mass below M_e.[57] The data suggest that the higher end group concentrations for lower molecular weight samples resulted in larger T_g enhancements. Similar behavior was observed in the ureido-4[1*H*]-pyrimidone functionalized polystyrenes.[25]

Conclusion

Novel uracil-containing alkoxyamines containing both TEMPO and DEPN were synthesized and used in the stable free radical polymerization of styrene and *n*-butyl acrylate. The resulting hydrogen bonding polymers exhibited narrow molecular weight distributions ($M_w/M_n \sim 1.20$) and controlled molecular weights, which are characteristic of stable free radical polymerizations. Linear progression of number-average molecular weight with conversion was observed. The rate constant of

n-butyl acrylate polymerization (3.7×10^{-5} s^{-1}) was slightly greater than k_{obs} for styrene polymerization (3.0×10^{-5} s^{-1}); however, it was lower than typical literature values probably due to the quantity of excess nitroxide present. Also, the styrene polymerization rate constant was higher than literature values possibly due to excess nitroxide which may be present in bimolecular systems but absent in unimolecular initiation.

Characterization of the polymers using ^{1}H NMR and melt rheology demonstrated the presence of the hydrogen bonding interaction. Furthermore, a stronger temperature dependence of melt viscosity was observed with uracil functionalized poly(*n*-butyl acrylate)s. Thermogravimetric analysis combined with pyrolysis experiments demonstrated that uracil−polystyrenes lost the TEMPO chain end during the first stage of degradation from 195 to 250 °C, however, that the uracil groups remained attached to the polymer chain end.

Acknowledgment. This material is based upon work supported by, or in part by, the U.S. Army Research Laboratory and the U.S. Army Research Office under Grant DAAD19-02-1-0275 Macromolecular Architecture for Performance (MAP) MURI.

Supporting Information Available: FTIR spectra for Uracil−TEMPO and Uracil−DEPN. This material is available free of charge via the Internet at http://pubs.acs.org.

References and Notes

(1) Hawker, C. J.; Bosman, A. W.; Harth, E. *Chem. Rev.* **2001**, *101*, 3661−3688.
(2) Matyjaszewski, K. *ACS Symp. Ser.* **2003**, *854*, 2−9.
(3) Hawker, C. J.; Hedrick, J. L.; Malmstrom, E.; Trollsas, M.; Stehling, U. M.; Waymouth, R. M. *ACS Symp. Ser.* **1998**, *713*, 127−139.
(4) Bisht, H. S.; Chatterjee, A. K. *J. Macromol. Sci., Polym. Rev.* **2001**, *41*, 139−173.
(5) Robin, S.; Guerret, O.; Couturier, J. L.; Pirri, R.; Gnanou, Y. *Macromolecules* **2002**, *35*, 3844−8.
(6) Pasquale, A. J.; Long, T. E. *J. Polym. Sci., Part A: Polym. Chem.* **2001**, *39*, 216−223.
(7) Bosman, A. W.; Vestberg, R.; Heumann, A.; Fréchet, J. M. J.; Hawker, C. J. *J. Am. Chem. Soc.* **2003**, *125*, 715−28.
(8) Hawker, C. J. *Acc. Chem. Res.* **1997**, *30*, 373−82.
(9) Solomon, D. H.; Rizzardo, P.; Cacioli, P. U.S. Pat. 4,581,429, 1986.
(10) Moad, G.; Rizzardo, E.; Solomon, D. H. *Macromolecules* **1982**, *15*, 909−914.
(11) Veregin, R. P. N.; Georges, M. K.; Kazmaier, P. M.; Hamer, G. K. *Macromolecules* **1993**, *26*, 5316−20.
(12) Benoit, D.; Chaplinski, V.; Braslau, R.; Hawker, C. J. *J. Am. Chem. Soc.* **1999**, *121*, 3904−20.
(13) Diaz, T.; Fischer, A.; Jonquieres, A.; Brembilla, A.; Lochon, P. *Macromolecules* **2003**, *36*, 2235−41.
(14) Benoit, D.; Harth, E.; Fox, P.; Waymouth, R. M.; Hawker, C. J. *Macromolecules* **2000**, *33*, 363−70.
(15) Le Mercier, C.; Lutz, J. F.; Marque, S.; Le Moigne, F.; Tordo, P.; Lacroix-Desmazes, P.; Boutevin, B.; Couturier, J. L.; Guerret, O.; Martschke, R.; Sobek, J.; Fischer, H. *ACS Symp. Ser.* **2000**, *748*, 108−122.
(16) Hawker, C. J.; Barclay, G. G.; Orellana, A.; Dao, J.; Devonport, W. *Macromolecules* **1996**, *29*, 5245−54.
(17) Wang, D.; Bi, X.; Wu, Z. *Macromolecules* **2000**, *33*, 2293−5.
(18) Dao, J.; Benoit, D.; Hawker, C. J. *J. Polym. Sci., Part A: Polym. Chem.* **1998**, *36*, 2161.
(19) Bothe, M.; Schmidt-Naake, G. *Macromol. Rapid Commun.* **2003**, *24*, 609−13.
(20) Matyjaszewski, K.; Woodworth, B. E.; Zhang, X.; Gaynor, S.; Metzner, Z. *Macromolecules* **1998**, *31*, 5955−7.
(21) Lange, R. F. M.; Van Gurp, M.; Meijer, E. W. *J. Polym. Sci., Part A: Polym. Chem.* **1999**, *37*, 3657−70.
(22) Müller, M.; Dardin, A.; Seidel, U.; Balsamo, V.; Iván, B.; Speiss, H. W.; Stadler, R. *Macromolecules* **1996**, *29*, 2577−83.
(23) Berl, V.; Schmutz, M.; Krische, M. J.; Khoury, R. G.; Lehn, J.-M. *Chem.−Eur. J.* **2002**, *8*, 1227−44.
(24) Yamauchi, K.; Lizotte, J. R.; Long, T. E. *Macromolecules* **2003**, *36*, 1083−8.
(25) Yamauchi, K.; Lizotte, J. R.; Hercules, D. M.; Vergne, M. J.; Long, T. E. *J. Am. Chem. Soc.* **2002**, *124*, 8599−604.
(26) Reith, L. R.; Eaton, R. F.; Coates, G. W. *Angew. Chem., Int. Ed.* **2001**, *40*, 2153−6.
(27) Nir, E.; Kleinermanns, K.; de Vries, M. S. *Nature (London)* **2000**, *408*, 949−51.
(28) Yamauchi, K.; Lizotte, J. R.; Long, T. E. *Macromolecules* **2002**, *35*, 8745−50.
(29) Ilhan, F.; Galow, T. H.; Gray, M.; Clavier, G.; Rotello, V. M. *J. Am. Chem. Soc.* **2000**, *122*, 5895−6.
(30) Inaki, Y. *Prog. Polym. Sci.* **1992**, *17*, 515−70.
(31) Khan, A.; Haddleton, D. M.; Hannon, M. J.; Kukulj, D.; Marsh, A. *Macromolecules* **1999**, *32*, 6560−4.
(32) Srivatsan, S. G.; Parvez, M.; Verma, S. *Chem.−Eur. J.* **2002**, *8*, 5184−91.
(33) Han, M. J.; Park, S. M.; Park, J. Y.; Yoon, S. H. *Macromolecules* **1992**, *25*, 3534−9.
(34) Inaki, Y.; Futagawa, H.; Takemoto, K. *J. Polym. Sci., Part A: Polym. Chem.* **1980**, *18*, 2959−69.
(35) Overberger, C. G.; Inaki, Y. *J. Polym. Sci., Part A: Polym. Chem.* **1979**, *17*, 1739−58.
(36) Han, M. J.; Chang, J. Y. *Adv. Polym. Sci.* **2000**, *153*, 1−36.
(37) Grimaldi, S.; Finet, J. P.; Le Moigne, F.; Zeghdaoui, A.; Tordo, P.; Benoit, D.; Fontanille, M.; Gnanou, Y. *Macromolecules* **2000**, *33*, 1141−47.
(38) Benoit, D.; Grimaldi, S.; Robin, S.; Finet, J. P.; Tordo, P.; Gnanou, Y. *J. Am. Chem. Soc.*, **2000**, *122*, 5929−39.
(39) Lacroix-Desmazes, P.; Lutz, J. F.; Chauvin, F.; Severac, R.; Boutevin, B. *Macromolecules* **2001**, *34*, 8866−71.
(40) Pasquale, A. J.; Lizotte, J. R.; Williamson, D. T.; Long, T. E. *Polym. News* **2002**, *27*, 272−283.
(41) Lizotte, J. R.; Long, T. E. *Macromol. Chem. Phys.* **2003**, *204*, 570−576.
(42) Lizotte, J. R.; Long, T. E. *Polym. Mater. Sci. Eng.* **2003**, *88*, 471−472.
(43) Lizotte, J. R.; Erwin, B. M.; Colby, R. H.; Long, T. E. *J. Polym. Sci., Part A: Polym. Chem.* **2002**, *40*, 583−590.
(44) Pasquale, A. J.; Long, T. E. *Macromolecules* **1999**, *32*, 7954. Value of k_{obs} was 2.09×10^{-5} s^{-1}.
(45) Moffat, K.; Hamer, G. K.; Georges, M. K. *Macromolecules* **1999**, *32*, 1004−1012.
(46) Fischer, A.; Brembilla, A.; Lochon, P. *Macromolecules* **1999**, *32*, 6069−72.
(47) Fukuda, T.; Terauchi, T.; Goto, A.; Ohno, K.; Tsujii, Y.; Miyamoto, T. *Macromolecules* **1996**, *29*, 6393−8.
(48) For example, in a dimeric system at equilibrium A + B ⇌ AB. Assume [A] = [B] and let M_0 designate the initial concentrations of each before mixing. Thus, the equilibrium concentration of the dimer [AB] = M_0x, where x is the fraction of conversion to the dimer. Then, [A] = [B] = $M_0(1 - x)$ so $K_a = x/(M_0(1 - x)^2)$ (eq 1). Dilution would have the same effect on equilibrium as starting with lower initial concentrations of [A] and [B] prior to mixing (M_0 decreases). To maintain the value of right-hand side of the eq 1, x must consequently decrease. LeChatelier's principle also suggests that dilution will diminish the concentration of the dimer.
(49) Chen, J. S.; Shirts, R. B. *J. Phys. Chem.* **1985**, *89*, 1643−46.
(50) Beijer, F. H.; Sijbesma, R. P.; Vekemans, J. A. J. M.; Meijer, E. W.; Kooijman, H.; Spek, A. L. *J. Org. Chem.* **1996**, *61*, 6371−80.
(51) Zheng, W.; Angelopoulos, M.; Epstein, A. J.; MacDiarmid, A. G. *Macromolecules* **1997**, *30*, 2953−55.
(52) Lillya, C. P.; Baker, R. J.; Huette, S.; Winter, H. H.; Lin, H.-G.; Shi, J.; Dickinson, L. C.; Chien, J. C. W. *Macromolecules* **1992**, *25*, 2076.
(53) Müller, M.; Dardin, A.; Seidel, U.; Balsamo, V.; Ivan, B.; Spiess, H. W.; Stadler, R. *Macromolecules* **1996**, *29*, 2577.
(54) Wilkes, G. L. *J. Chem. Educ.* **1981**, *58*, 880−892.
(55) Roland, A. I.; Schmidt-Naake, G. *J. Anal. App. Pyrol.* **2001**, *58−9*, 143−54.
(56) Fetters, L. J.; Lohse, D. J.; Milner, S. T. *Macromolecules* **1999**, *32*, 6847−51.
(57) Lin, Y. H. *Macromolecules* **1990**, *23*, 5292−94.

MA048938Q